

## Fused Deposition Modelling as an Effective Tool for Anti-Infective Dialysis Catheter Fabrication

Essyrose Mathew, Juan Domínguez-Robles, Sarah Stewart, Elena Mancuso, Kieran O'Donnell, Eneko Larraneta, and Dimitrios A. Lamprou

*ACS Biomater. Sci. Eng.*, **Just Accepted Manuscript** • DOI: 10.1021/  
acsbiomaterials.9b01185 • Publication Date (Web): 23 Sep 2019

Downloaded from [pubs.acs.org](https://pubs.acs.org) on September 23, 2019

### Just Accepted

“Just Accepted” manuscripts have been peer-reviewed and accepted for publication. They are posted online prior to technical editing, formatting for publication and author proofing. The American Chemical Society provides “Just Accepted” as a service to the research community to expedite the dissemination of scientific material as soon as possible after acceptance. “Just Accepted” manuscripts appear in full in PDF format accompanied by an HTML abstract. “Just Accepted” manuscripts have been fully peer reviewed, but should not be considered the official version of record. They are citable by the Digital Object Identifier (DOI®). “Just Accepted” is an optional service offered to authors. Therefore, the “Just Accepted” Web site may not include all articles that will be published in the journal. After a manuscript is technically edited and formatted, it will be removed from the “Just Accepted” Web site and published as an ASAP article. Note that technical editing may introduce minor changes to the manuscript text and/or graphics which could affect content, and all legal disclaimers and ethical guidelines that apply to the journal pertain. ACS cannot be held responsible for errors or consequences arising from the use of information contained in these “Just Accepted” manuscripts.

1  
2  
3 **Fused Deposition Modelling as an Effective Tool for Anti-Infective Dialysis Catheter**  
4 **Fabrication**  
5

6 Essyrose Mathew,<sup>1,⊥</sup> Juan Domínguez-Robles,<sup>1,⊥</sup> Sarah A. Stewart,<sup>1</sup> Elena Mancuso,<sup>2</sup> Kieran  
7 O'Donnell,<sup>2</sup> Eneko Larrañeta,<sup>1,\*</sup> Dimitrios A. Lamprou<sup>1,\*</sup>  
8  
9

10  
11 <sup>1</sup> School of Pharmacy, Queen's University Belfast, 97 Lisburn Road, Belfast BT9 7BL, UK  
12

13 <sup>2</sup> Nanotechnology and Integrated Bio-Engineering Centre (NIBEC), Ulster University,  
14 Jordanstown campus, UK  
15

16 <sup>⊥</sup>These authors contributed equally to this work  
17  
18  
19  
20  
21  
22  
23

24 **Corresponding authors:**  
25

26 \*School of Pharmacy, Queen's University Belfast, 97 Lisburn Road, Belfast BT9 7BL, UK  
27

28 [e.larraneta@qub.ac.uk](mailto:e.larraneta@qub.ac.uk)  
29

30 [d.lamprou@qub.ac.uk](mailto:d.lamprou@qub.ac.uk)  
31  
32  
33  
34  
35  
36  
37  
38  
39  
40  
41  
42  
43  
44  
45  
46  
47  
48  
49  
50  
51  
52  
53  
54  
55  
56  
57  
58  
59  
60

1  
2  
3  
4  
5 **Abstract:** Catheter associated infections are a common complication that occurs in dialysis  
6 patients. Current strategies to prevent infection include catheter coatings containing heparin,  
7 pyrogallol or silver nanoparticles, which all have an increased risk of causing resistance in  
8 bacteria. Therefore, a novel approach for manufacture, such as the use of additive  
9 manufacturing (AM), also known as 3D-printing, is required. Filaments were produced by  
10 extrusion using thermoplastic polyurethane (TPU) and Tetracycline Hydrochloride (TC) in various  
11 concentrations (e.g. 0%, 0.25%, 0.5% and 1%). The extruded filaments were used in a fused  
12 deposition modelling (FDM) 3D-printer to print catheter constructs at varying concentrations.  
13 Release studies in phosphate buffered saline (PBS), microbiology studies, thermal analysis,  
14 contact angle, ATR-FTIR, scanning electron microscopy (SEM) and X-ray Micro Computer  
15 Tomography ( $\mu$ CT) analysis were conducted on the printed catheters. The results suggested that  
16 TC was uniformly distributed within the TPU matrix. The microbiology testing of the catheters  
17 showed that devices containing TC had an inhibitory effect on the growth of *Staphylococcus*  
18 *aureus* NCTC 10788 bacteria. Catheters containing 1% TC maintained inhibitory effect after  
19 10-day release studies. After an initial burst release in the first 24 h, there was a steady release  
20 of TC in all concentrations of catheters. 3D-printed antibiotic catheters were successfully printed  
21 with inhibitory effect on *S. aureus* bacteria. Finally, TC containing catheters showed resistance  
22 to *S. aureus* adherence to their surfaces when compared with catheters containing no TC.  
23 Catheters containing 1% of TC showed a bacterial adherence reduction of up to 99.97%.  
24 Accordingly, the incorporation of TC to TPU materials can be effectively used to prepare anti-  
25 infective catheters using FDM. This study highlights the potential for drug impregnated medical  
26 devices to be created through AM.  
27  
28  
29  
30  
31  
32  
33  
34  
35  
36  
37  
38  
39  
40  
41  
42  
43  
44  
45

46 **Keywords:** 3D-printing; Additive Manufacturing; Fused Deposition Modelling; Extrusion;  
47 Catheters; Dialysis; Drug Release.  
48  
49  
50  
51  
52  
53  
54  
55  
56  
57  
58  
59  
60

## 1. Introduction

Additive manufacturing (AM), also known as 3D-printing, is an area which has gained a lot of interest in recent years due to its wide range of applications.<sup>1-3</sup> 3D-printing, allows a model which is created using computer aided design to be formed into a physical object. For this purpose, a wide variety of materials can be used, ranging from synthetic polymers to biomolecules.<sup>3-7</sup> Due to this, AM has a wide variety of applications in diverse fields ranging from aerospace engineering to medical applications.<sup>4</sup> AM includes a wide variety of different types of techniques. All these techniques use different types of substrates such as resins, powders, gels or ceramics among others.<sup>8</sup> However, they all have one thing in common, they produce 3D object adding material layer by layer.<sup>8</sup> One of the most common and inexpensive types of AM is fused deposition modelling (FDM). FDM requires the use of a polymeric filament that is pushed through a hot nozzle to melt the polymer and, subsequently, generating the required object.<sup>8</sup>

Diverse medical applications of 3D-printing have been described including orthopaedics, tissue engineering or the manufacture of medical devices.<sup>9-13</sup> 3D-printing technology allows design and fabrication of structures based on images captured from patients with medical imaging techniques (i.e. magnetic resonance imaging (MRI) or computer tomography (CT)).<sup>3</sup> Accordingly, 3D-printing can be used to prepare medical devices adapted to a particular patient's needs. Conventional fabrication techniques cannot offer this versatility.

Biocompatible materials such as poly(lactic acid) or thermoplastic polyurethane (TPU) have been used extensively for 3D-printing applications.<sup>4,14-16</sup> This polymer very desirable for medical applications due to its resiliency, inertness in the body and blood compatibly.<sup>17</sup> Moreover, it has been previously used for healthcare 3D printing applications such as the preparation of bolus for radiation therapy<sup>18-20</sup> or the development of stents for enterocutaneous fistula surgery.<sup>21</sup> The later work shows not only that the material is biocompatible, but also that 3D printing of TPU devices can be prepared for patient benefit.

One potential application of 3D-printing is the manufacture of medical devices such as catheters,<sup>22</sup> as it opens up the potential for creating patient matched devices specific to their anatomy. This would allow the potential for on demand patient matched devices to be created in hospital settings. Moreover, the versatility of 3D-printing to use different types of materials can be used to add drugs, such as antibiotics, to the resulting structure.<sup>6,23,24</sup> This is interesting for catheter manufacturing due to the tendency of these medical devices to be colonised by bacteria. A high percentage of catheter-related infections occur due to gram positive bacteria such as *Staphylococcus aureus*.<sup>25</sup> This is especially problematic for dialysis catheters.

1  
2  
3 Catheter-related infections (CRI) in dialysis patients are the second major cause of death among  
4 these patients and significantly increase the treatment cost.<sup>26,27</sup> *Staphylococcus aureus* in  
5 Haemodialysis (HD) patients and *Staphylococcus aureus* and *Pseudomonas aeruginosa* in  
6 peritoneal dialysis (PD) patients are the most common causative organisms isolated. Patients  
7 with CRI are hospitalised more frequently than the general population, and CRI contributes to  
8 the higher associated mortality of dialysis patients compared to the general population.  
9 Considering that in the UK around 30,000 people are receiving dialysis treatment,<sup>28</sup> it is  
10 estimated that catheter related infections of these patients are costing the UK National Health  
11 Service (NHS) ca. £1.4 million per year.<sup>27</sup> Accordingly, the use of 3D-printing has potential to  
12 manufacture anti-infective catheters adapted to patient's needs.

13  
14  
15  
16  
17  
18  
19  
20  
21 In the present work, FDM will be explored for first time to our knowledge, to prepare catheters  
22 containing tetracycline (TC) to prevent bacterial colonisation of the resulting catheters. FDM  
23 works by extruding a polymer in successive layers onto a build plate where it is then cooled and  
24 solidified. For this purpose, the selected polymer was TPU, a flexible polymer that has been  
25 extensively used for biomedical applications (including catheter manufacturing).<sup>29–32</sup> Before  
26 printing the catheters prototypes, TPU filaments containing the antibiotic were required.  
27 Accordingly, hot-melt extrusion (HME) was used to prepare these filaments. The resulting  
28 catheters were characterised by a variety of microscopic and spectroscopic techniques, and their  
29 antimicrobial properties were evaluated.

## 30 31 32 33 34 35 36 **2. Experimental Section**

### 37 38 39 **2.1. Materials**

40  
41 Elastollan<sup>®</sup>, thermoplastic polyurethane (TPU) elastomer pellets with 75A shore hardness were  
42 kindly provided by DISTRUPOL Ltd (Dublin, Ireland). Tetracycline Hydrochloride (TC) drug was  
43 purchased from Sigma Aldrich, (Dorset, UK). Castor oil was obtained from Ransom (Hitchin, UK).  
44 Phosphate Buffer Solution (PBS) at pH 7.4 prepared using PBS tablets Merck (Darmstadt,  
45 Germany).

46  
47  
48  
49  
50 *Staphylococcus aureus* NCTC 10788 was maintained on cryopreservative beads in 10% glycerol  
51 at -80°C and grown in Luria-Bertani (LB) broth or Mueller-Hinton Broth (MHB) at 37°C when  
52 required for the microbiological assessments. Moreover, to perform the different *in vitro*  
53 microbiological assays, several broths and solutions were used. For the zone of inhibition assay,  
54 LB agar and LB soft agar were used. Additionally, for the *in vitro* adherence assay Mueller-Hinton  
55 agar (MHA) and tryptone soya broth (TSB), as well as quarter-strength Ringers Solution (QSRS)  
56 and PBS were used.

## 2.2. Preparation of TC Containing TPU filaments and catheters

HME was used to combine the drug and polymer in order to create filaments which would be used for 3D-printing. To ensure an even coating of TC on the surface of the TPU pellets, an oil method for coating was used.<sup>23</sup> Briefly, a 50 mL Falcon tube was filled with TPU pellets (40 g). Then, castor oil (40  $\mu$ L) was added into the tube and it was vortexed until the pellets were properly coated. Subsequently, these oil coated pellets were transferred to a new 50 mL Falcon tube to avoid loss of drug, by sticking to leftover oil, on the walls of tube. TC was then added in ratios of 0.25% w/w, 0.5% w/w and 1% w/w and vortexed to evenly coat all pellets. Coated pellets were added to filament extruder (3Devo, Utrecht, The Netherlands) at extrusion speed of 5 rpm and filament fan speed of 90%. Finally, the temperature was adjusted through a control panel positioned at the side of the extruder and it was between 170 and 190°C, due to the existence of 4 heaters.

## 2.3. Preparation of TC Containing Catheters Using 3D-Printing.

Once the filaments were extruded, catheters with 5 mm external diameter and 2mm internal diameter, as well as squares of 10 mm x 10 mm x 1 mm were 3D-printed using an Ultimaker 3 (Ultimaker B.V., Geldermalsen, The Netherlands) fused filament fabrication (FFF) system and Cura<sup>®</sup> software. The Ultimaker 3 FFF system was equipped a 0.4 mm nozzle. It is important to note that this equipment is a RepRap Open Source FFF equipment.<sup>33</sup> The optimised printing parameters can be seen in Table 1.

**Table 1.** 3D printing parameters used for catheter production.

Print-head temperature (°C)	Bed temperature (°C)	Layer height (mm)	Speed (mm/s)	Infill density (%)
215	60	0.1	12	100

## 2.4. Characterisation of TPU filaments and 3D printed catheters.

### 2.4.1. Microscopy

The morphologies of the filaments and the 3D printed catheters were assessed using a Leica EZ4 W digital microscope (Leica, Wetzlar, Germany). The microscope was equipped with fluorescence filters (excitation 440–460 nm and emission 500 nm) (Nightsea, Lexington, MA, USA) to evaluate the distribution of TC within the filaments. Moreover, the surface morphology of the 3D-printed catheters containing TC (0.25, 0.5 and 1.0%) and without TC, before and after the 10-days

1  
2  
3 release study were analysed using Scanning Electron Microscope (SEM) (Hitachi TM3030, Tokyo,  
4 Japan).

#### 6 7 *2.4.2. Mechanical properties*

9 TA.XTplus texture analyser (Stable Micro Systems, Surrey, UK) was used to evaluate the elastic  
10 modulus and the fracture force of the resulting filaments. Pieces of filament of 6 cm were cut  
11 and clamped vertically into the texture analyser. The distance between both clamps was 2 cm.  
12 The filament was vertically stretched at a rate of 50 cm/min. The texture analyser stretched the  
13 filament up to 20 cm. Subsequently the elastic modulus was calculated from the slope from the  
14 obtained stress/strain curves.  
15  
16  
17  
18

#### 19 20 *2.4.3. Infrared Spectroscopy*

21 The Fourier Transform Infrared (FTIR) spectra of the resulting TC containing TPU materials were  
22 recorded using a Spectrum Two™ instrument (Perkin Elmer, Waltham, MA, USA) by the  
23 attenuated total reflectance (ATR) technique. The spectra were recorded from 4000 cm<sup>-1</sup> to  
24 600 cm<sup>-1</sup> with a resolution of 4 cm<sup>-1</sup> and a total of 16 scans were collected.  
25  
26  
27  
28

#### 29 30 *2.4.4. Thermogravimetric analysis*

31 As the elastomer is exposed to high temperatures during the printing process, the thermal  
32 degradation behaviour of the polymer was examined. Thermogravimetric analysis (TGA) was  
33 performed to measure the weight loss of the TC containing TPU materials. For this purpose,  
34 small fragments of the filaments containing 0% and 1% TC concentration were used. TGA was  
35 performed on a Q500 Thermogravimetric analysis (TA instruments, Bellingham, WA, USA). Scans  
36 were run from room temperature to 550°C, at a heating rate of 10°C/min under a nitrogen flow.  
37  
38  
39  
40  
41  
42

#### 43 44 *2.4.4. Contact angle*

45 The contact angle of water with the surface of the resulting TC containing TPU materials was  
46 evaluated using an Attension Theta equipment (Attension Theta, Biolin Scientific, Gothenburg,  
47 Sweden). OneAttension software analysed results to give an indication of the wettability of the  
48 surface.  
49  
50  
51

#### 52 53 *2.4.4. X-ray microcomputer tomography*

54 X-ray Micro Computer Tomography (μCT) scans were also performed on 3D-printed catheters.  
55 A Bruker Skyscan 1275, with a Hamamatsu L11871 source (40kV, 250μA) and 3 MP active pixel  
56 CMOS flat panel detector was used. Samples were mounted vertically on dental wax and  
57 positioned 59.791 mm from the source, where camera to source distance was 286 mm. No filter  
58  
59  
60

1  
2  
3 was applied for an exposure time of 49 ms. The images generated were 1944x1413 pixels with  
4 a resolution of 17  $\mu\text{m}$  per pixel. A total of 1056 images were taken in 0.2° steps around one  
5 hemisphere of the sample, with an average of 3 frames taken at each rotation step.  
6  
7

8  
9 The images were collected, and subsequently a volumetric reconstruction of each sample was  
10 generated using Bruker's CTvol software. Attenuation thresholding was conducted manually, in  
11 order to eliminate speckle around the samples. The same thresholding was applied within  
12 Bruker's CTan software, where the samples were further processed.  
13  
14

## 15 16 **2.5. TC release Study**

17  
18 A release study was performed to calculate the amount of TC eluting from the resulting  
19 catheters. Catheters were placed in Eppendorf's containing 1 mL of PBS which were placed in a  
20 shaking incubator at 37°C and 40 rpm. Samples were taken at predetermined time intervals  
21 (each 24 h for 10 days). Catheters were removed from the Eppendorf's, dried and transferred to  
22 new Eppendorf's containing 1 mL of fresh PBS. The concentration of TC was evaluated using a  
23 UV-visible plate reader (PowerWave XS Microplate Spectrophotometer, Bio-Tek, Winooski, VT,  
24 USA) at a wavelength of 363 nm.  
25  
26  
27  
28  
29

## 30 31 **2.6. *In Vitro* Microbiological Analysis**

32  
33 Printed catheters were tested for inhibitory effect on a bacterial culture of *S. aureus*. For this  
34 purpose, catheters at each concentration (0 -1% of TC) were cut into 4 x 2 mm discs using a  
35 scalpel. Two sets of catheters discs were tested. Catheters that were used directly after  
36 3D-printing were referred to as unwashed (UW) catheters, and catheters that were submitted  
37 to a release in PBS media for 10 days were referred to as washed (W) catheters. Then, UW and  
38 W catheter discs were placed in a Class II Microbiological Safety Cabinet (BioMAT2) and left  
39 under UV light for 30 min on each side of the disc to be sterilised. To perform this experiment,  
40 80  $\mu\text{L}$  of a saturated culture of *S. aureus* was added to 5 mL of Luria-Bertani (LB) soft agar. This  
41 mixture was then poured on top of the LB agar plate. Catheter discs were placed in the centre  
42 of the plate and incubated for 24 hours at 37°C. The inhibition zone diameters were then  
43 measured in mm. Furthermore, three inoculated plates with no catheter discs were also  
44 incubated as a positive control.  
45  
46  
47  
48  
49  
50  
51  
52

53  
54 Additionally, an *in vitro* assay of bacterial adhesion onto these printed catheters was performed.  
55 For this purpose, squares (with the following dimensions: 1cm x 1cm x 0.1cm) were 3D-printed  
56 using the same filaments as for the catheters containing 0%, 0.25%, 0.5% and 1% TC. This  
57 analysis was carried out in accordance with previous published work.<sup>34,35</sup> In brief, a bacterial  
58  
59  
60



1  
2  
3 suspension of *S. aureus* ( $1 \times 10^8$  cfu mL<sup>-1</sup>) in PBS and supplemented with 0.5% TSB (pH 7), was  
4 diluted (1:100) with PBS containing 0.5% TSB. Replicate samples of the abovementioned  
5 3D-printed squares were placed in individual wells of a sterile 24-well plate containing 1 mL of  
6 the respective bacterial suspension with a density of  $1 \times 10^6$  cfu mL<sup>-1</sup>. The plate was continuously  
7 shaken in an orbital incubator at 37°C for 24 hours. The samples were then removed from the  
8 24-well plate containing the bacterial suspension and the nonadherent bacteria were removed  
9 by serial washing, first in PBS (1 x 10 mL), and secondly, in QSRS (3 x 10 mL).<sup>36</sup> Samples were  
10 then transferred into fresh QSRS (5mL), sonicated for 15 min and vortexed for 30 s to remove  
11 adherent bacteria. The sonication technique has previously been demonstrated not to affect  
12 bacterial viability or morphology.<sup>37</sup> A viable count of the QSRS was performed by the Miles and  
13 Misra serial dilution technique<sup>38</sup> followed by plating onto Mueller-Hinton agar to enumerate the  
14 previously adhered bacteria per sample. Percentage reductions in the number of adherent  
15 bacteria to each sample (UW and W catheters containing 0.25%, 0.5% and 1% TC) relative to the  
16 control samples (UW and W catheters containing 0% TC) were calculated.

## 27 **2.7. Statistical Analysis**

28  
29 Quantitative data was expressed as a mean  $\pm$  standard deviation, n=3. The statistical analysis  
30 was performed using a one-way analysis of variance (ANOVA),  $p < 0.05$  was considered to be  
31 statistically significant.

## 35 **3. Results and Discussion**

### 37 **3.1. Preparation and Characterisation of TC Containing TPU Materials**

38  
39 Extrusion of the TPU pellets containing the different TC concentrations produced smooth  
40 filaments of 2.85 mm in diameter (Figure 1A). Moreover, the colour of the filament darkened as  
41 the mass of TC added increased, confirming that an increased amount of TC is present in the  
42 extruded filaments. It can be inferred that the TC was mixed successfully with the TPU matrix.  
43 This can be confirmed by microscopy (Figure 1A), which show that TC was dissolved in the  
44 molten TPU within the extruder, as the filaments are homogeneous showing no visible TC  
45 aggregates. Moreover, fluorescence images did not show any TC aggregate within the material  
46 (Figure 1B). Additionally, Figure 1C shows the cross section of the filaments. The filaments  
47 showed homogeneous distribution of TC along the filament and accordingly this suggest that  
48 the mixing process in the extrusion was successful and that the drug and the polymer should be  
49 dissolved within the TPU matrix. Moreover, this can be confirmed by SEM, Figure S1 (supporting  
50 information). These SEM images of the cross section of blank TPU and TPU containing 1% of TC  
51 filaments showed no visible TC crystals or aggregates in the filaments.

1  
2  
3 The good miscibility between TPU and TC can be explained by their chemical structures. The TPU  
4 used in the present work contains aromatic groups within its polyurethane units.<sup>39</sup> On the other  
5 hand, TC contains a linear fused tetracyclic nucleus structure including a benzene ring and  
6 multiple conjugated double bonds.<sup>40</sup> Accordingly, the interaction between the aromatic  
7 moieties of TPU and TC can explain the good miscibility between these two compounds. The  
8 interactions between TPU and TC have been previously reported by Okoli *et al.*<sup>41</sup> These reported  
9 interactions were based on  $\pi$ - $\pi$  interactions between the aromatic moieties within TPU and TC.

10  
11  
12  
13  
14  
15 TPU filaments prepared containing TC were tested to evaluate if the presence of TC influenced  
16 their mechanical properties. Figure 1D shows the elastic modulus of the filaments as a function  
17 of the TC content. It is noticeable that the presence of TC did not alter the elastic modulus of  
18 the materials ( $p > 0.05$ ). Moreover, the filaments were stretched up to 2000% of the initial  
19 length. None of the tested specimens fractured during the test.

20  
21  
22  
23  
24 To the best of our knowledge, there is no report of this type of TPU being used for 3D-printing  
25 applications. However, Christ *et al.* described the use of TPU Elastollan 1185A, a similar type of  
26 TPU, reinforced with carbon nanotubes for 3D-printing applications.<sup>42</sup> The obtained elastic  
27 modulus for these filaments were higher than the ones reported here. However, this type of  
28 TPU has a higher shore hardness (85A vs 70A) and higher inherent elastic modulus. Moreover,  
29 the addition of 1% of carbon nanotubes to the TPU significantly increased the elastic modulus  
30 by more than a 50%. Interestingly, the presence of 1% of TC did not alter the elastic modulus of  
31 the filaments. Considering that TC was dissolved within the TPU during the extrusion, it can be  
32 concluded that there are interactions between the drug and the polymer. However, the results  
33 obtained suggest that the amount of drug incorporated into the polymers was not alter the  
34 mechanical properties of the material.

35  
36  
37  
38  
39  
40  
41  
42  
43  
44  
45  
46  
47  
48  
49  
50  
51  
52  
53  
54  
55  
56  
57  
58  
59  
60  
FTIR spectroscopy was used to evaluate if there were any interaction between TPU and TC  
(Figure 1E). The FTIR of TC showed peaks assigned to O-H (ca. 3460  $\text{cm}^{-1}$ ), N-H (ca. 3450  $\text{cm}^{-1}$ ),  
C=O (1600-1700  $\text{cm}^{-1}$ ) and =C-N (ca.1460  $\text{cm}^{-1}$ ) bonds.<sup>43</sup> On the other hand, TPU showed the  
characteristic peaks for the urethane group (C=O stretching vibration ca. 1700  $\text{cm}^{-1}$  and N-H  
vibrations 3300-3400  $\text{cm}^{-1}$ ).<sup>44</sup> The FTIR spectra of TPU containing 1% of TC did not any of the  
characteristic TC peaks or any peak shift. This could be due to the low drug content of the  
materials. However, it is obvious by the colour of the resulting materials (Figure 1A-1C) that the  
drug was blended in the TPU matrix. These results are similar to the ones obtained by Okoli *et al.*<sup>41</sup>  
This work described the development of a TPU-based magnetic composite for TC removal  
from aqueous environments. In this work, the only reported changes in the FTIR spectra were

1  
2  
3 related with the interactions between TC and the Fe within the structure. No other FTIR peaks  
4 showed changes that can suggest any interactions between TPU and TC.  
5  
6

7 FTIR spectroscopy and mechanical testing were not showing differences between TPU and TC  
8 containing materials. Accordingly, thermal analysis was performed to establish if there were any  
9 interactions between TC and TPU. TGA analysis of TPU and TPU containing 1% of TC showed  
10 differences between these two materials (Figure 1F). The material containing TC showed an  
11 improved thermal resistance. For this purpose, the onset temperatures ( $T_{\text{onset}}$ ) for both materials  
12 were measured.  $T_{\text{onset}}$  denotes the temperature at which the weight loss begins. As can be seen  
13 in Figure 1F, the  $T_{\text{onset}}$  of the TPU is shifted to a higher  $T_{\text{onset}}$  (from 306.5 to 322.7°C) after the  
14 addition of 1% of TC (1%). This is largely due to the existing interaction between the drug and  
15 the TPU polymeric matrix. These results suggest that there are interactions between TC and TPU.  
16 TC is preventing TPU degradation. Similar results were reported before when TPU was combined  
17 with Schiff base additives.<sup>44</sup> These compounds acted as flame retardant when combined with  
18 TPU. Hydrogen bonding interactions of O-H groups in the Schiff base compounds with the C=O  
19 of the urethane group in TPU were reported. TC has multiple O-H groups capable of establishing  
20 this type of interaction.  
21  
22  
23  
24  
25  
26  
27  
28  
29  
30

31 Finally, water contact angle with TPU and TC loaded TPU materials was evaluated (Figure 1G).  
32 The obtained values ranged between 90 and 105°. Accordingly, it can be established that all the  
33 prepared materials were hydrophobic in nature as water contact angle values were higher than  
34 90°. <sup>45</sup> No significant differences were obtained between all the TC containing TPU materials  
35 ( $p > 0.05$ ). However, the contact angle showed lower values when the TC concentration was  
36 increased from 0.5 to 1%. In the present study, TC was used in its hydrochloride salt form.  
37 Accordingly, this drug is a hydrophilic drug. This explains why materials containing higher TC  
38 loadings showed “lower” hydrophilicity.  
39  
40  
41  
42  
43  
44  
45  
46  
47  
48  
49  
50  
51  
52  
53  
54  
55  
56  
57  
58  
59  
60

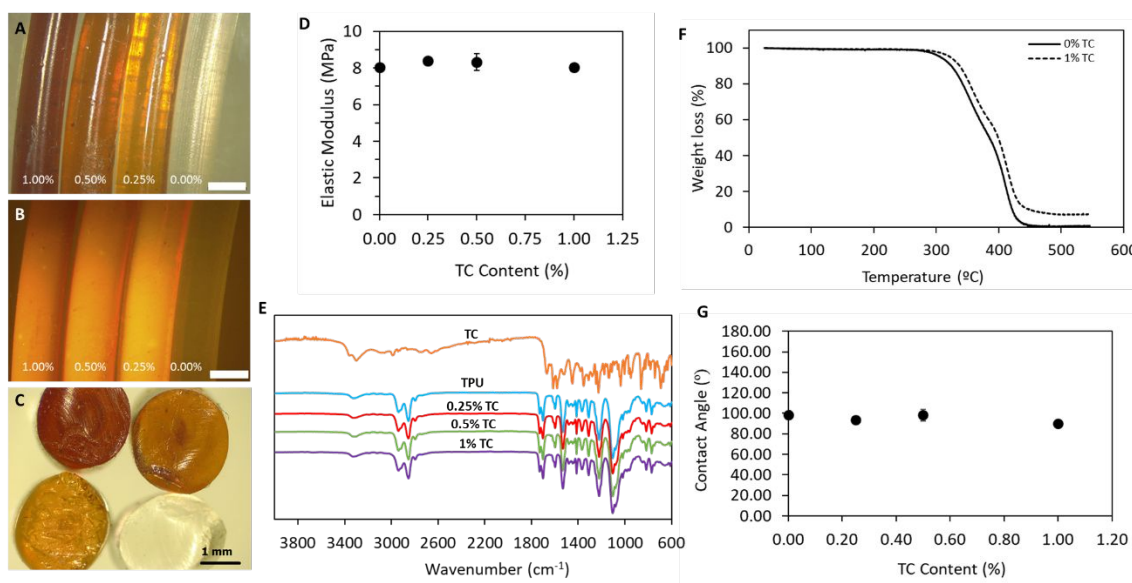


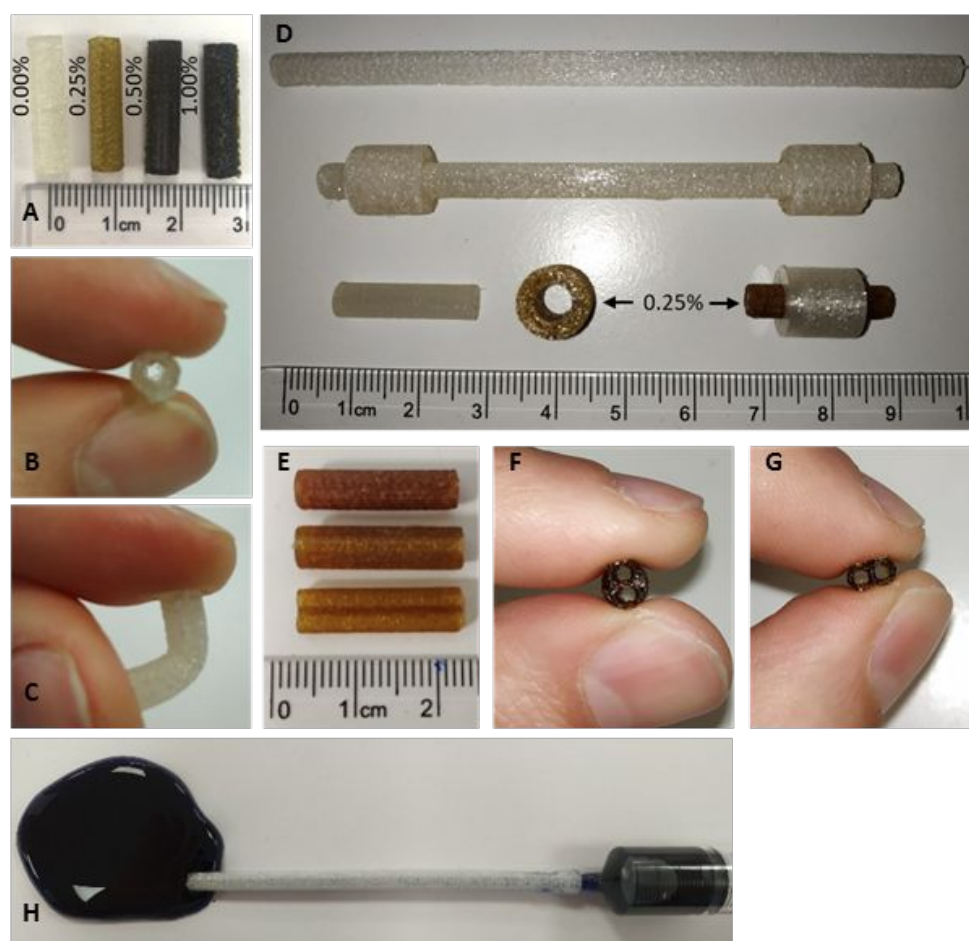
**Figure 1** (A). Microscopy (A) and fluorescent microscopy (B) images of TPU filaments containing 0%, 0.25%, 0.5% and 1% of TC. Cross section microscopy image of the filaments (C). Elastic modulus of the TC containing filaments (D). FTIR-ATR of TC containing TPU materials (E). TG curves TC containing TPU materials (0% and 1% TC) (F). Contact angle of water with the surface of TC containing TPU materials (G).

### 3.2. Preparation of TC Containing Catheters Using 3D-Printing.

TPU and TPU/TC filaments were used to produce catheters using fused deposition modelling. Figure 2 shows fragments of catheters produced with the previously mentioned materials. It can be seen that catheters containing higher TC loadings showed darker colours (Figure 2A). Moreover, due to the inherent flexibility of TPU the resulting catheters were flexible (Figure 2B and 2C). Central venous lines require the presence of cuffs to provide stability once they are in place. Figure 2D shows that the technique can be used to prepare more sophisticated catheters such as cuffed catheters. Moreover, FDM can be used to prepare independent cuffs with and without antibiotic (Figure 2D). The development of antiseptic cuffs to prevent catheter-related infections has been previously described.<sup>46</sup> However, the literature report that the most used bactericidal agent for this purpose was silver and it showed limited effectivity.<sup>47,48</sup> Accordingly, we believe that the use of antibiotic, such as TC, will significantly reduce bacterial colonisation of the material. The results showed in the present paper are a proof of concept and, accordingly, the catheters used for further studies were on lumen catheters. However, catheters used for HD or central venous lines present more complex designs including more than one lumen.<sup>49</sup> Figure 2E-2G shows that FDM can be used to prepare these types of designs. Finally, it is important to note that liquid can flow through the catheters without leaking. To illustrate this a methylene

1  
2  
3 blue solution was injected through a 3D printed catheter (Figure 2H). During the process, no  
4 leakage was observed.  
5  
6

7  
8 The use of 3D-printing catheters has been described before.<sup>22,24</sup> However, these publications  
9 described the concept and showed some examples of catheters prepared using poly(lactic acid)  
10 (PLA),<sup>23,24</sup> a commonly used 3D-printing material. This is not a good material for this application  
11 as full catheters cannot be produced using this material as it is not flexible. Realistically, these  
12 catheters cannot be used in patients.<sup>22</sup> The catheters described here are flexible (Figure 2) as  
13 they are made of TPU. This is the same material that is used to prepare catheters and central  
14 venous lines.<sup>50</sup> Moreover, FDM allows the on demand preparation of catheters and adaption  
15 to the needs of the patient. This is especially interesting for children that require catheters with  
16 non-conventional sizes.<sup>51</sup>  
17  
18  
19  
20  
21  
22



23  
24  
25  
26  
27  
28  
29  
30  
31  
32  
33  
34  
35  
36  
37  
38  
39  
40  
41  
42  
43  
44  
45  
46  
47  
48  
49  
50  
51  
52  
53  
54  
55  
56  
57  
58  
59  
60  
**Figure 2.** Catheters produced by Ultimaker3 Printer at concentrations of 0%, 0.25%, 0.5% and 1% TC showing their flexibility (A, B and C). Longer catheters with and without integrated cuffs, and spare printed cuffs with and without antibiotics (D). Different designed catheters used for dialysis and central venous lines (with two lumens) (E). Injection of a methylene blue solution (0.5mg/mL) through a TPU catheter.

SEM was used to characterise the surface of the printed catheters. These images show smooth uniform layers in the images before release (Figure 3). As can be seen in the Figure 3, there were no visible modifications in the layered structure of the catheters after the release study. FDM is an AM technique that creates 3D objects by sequential layer deposition.<sup>52</sup> SEM images showed the layers of the catheters printed using this technique. No differences are observed between blank catheters and TC loaded catheters.

The surface of the catheter's present certain degree of roughness and some minor defects. However, the prepared catheters did not leak as shown in Figure 2H. The work described here is a proof of concept and more work need to be developed before these materials can be used in real patients. One of the key aspects that can be improved for future developments is the surface roughness. There are different techniques that can be applied to improve it. The easiest one is use solvent vapour to smooth the surface of the prints.<sup>53</sup> However, this adds an additional step to the process and it is not ideal. An alternative to this is to implement alternative ways of printing. Nonplanar 3D printing can be used to obtain smoother surfaces.<sup>54,55</sup> This is not a new type of 3D printing but a new software algorithm to treat computer generated objects before printing. Accordingly, this novel software technique can be implemented in conventional FDM printers.

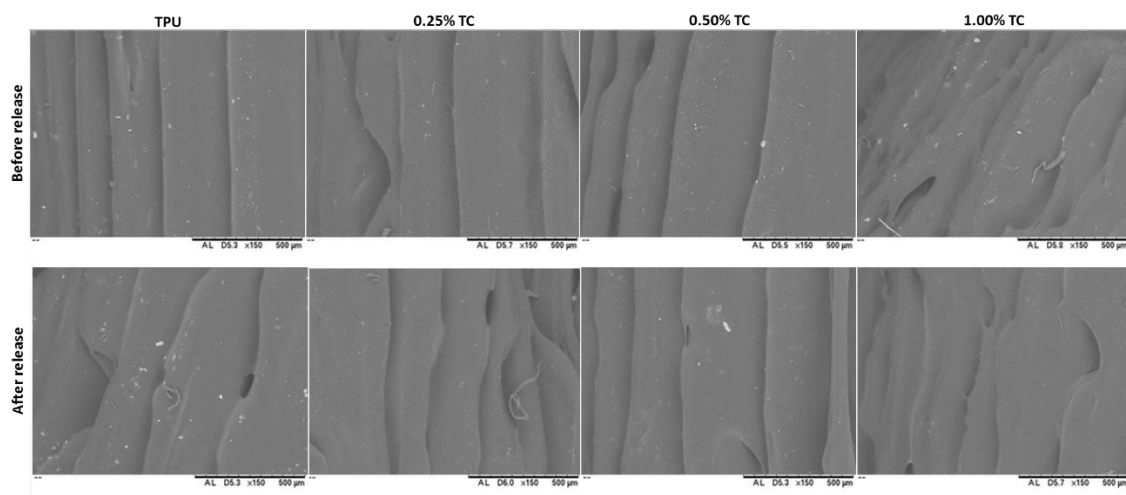
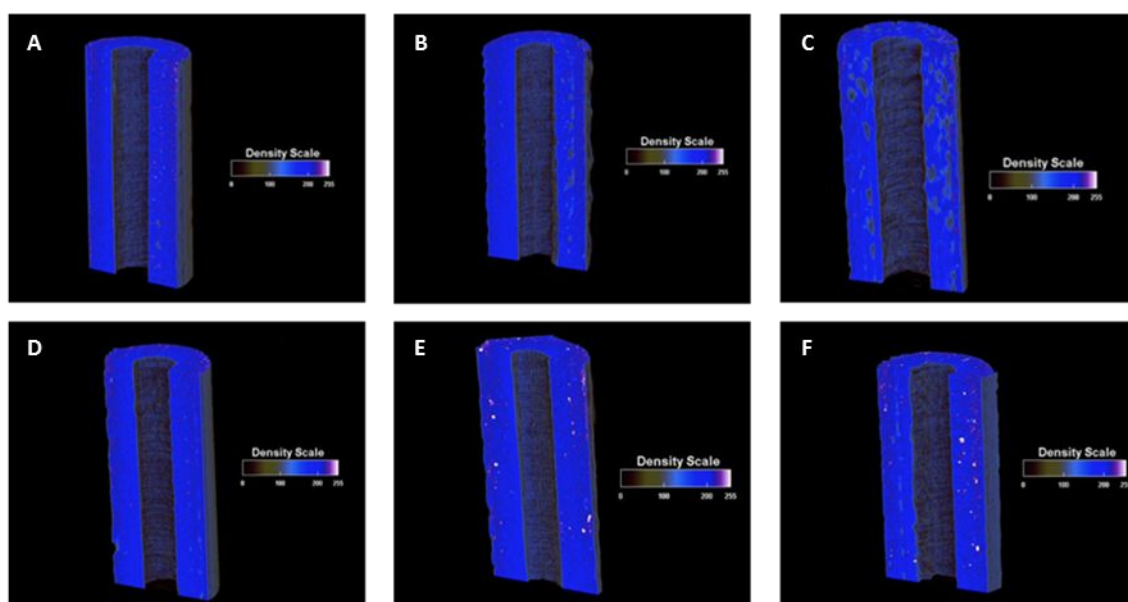


**Figure 3.** SEM micrography of 3D-printed catheters at concentrations of 0%, 0.25%, 0.5% and 1% before and after the release study. The scale bar represents 500 μm.

The 3D-printed sample architectures and topologies were analysed through the Bruker Skyscan 1172 system  $\mu$ CT. As it could be seen in the 3D volume reconstruction (Figure S2 in the supplementary material section), performed by using the Bruker's CTvol software, the drug incorporation did not affect the morphology of the 3D-printed samples, which were very similar

1  
2  
3 for all TC concentrations. In addition, even at the highest drug concentration (Figure S2E-S2F) all  
4 the samples were characterised by a continuous outer shell. In accordance to other studies  
5 published in the literature,<sup>56-58</sup> and where similar manufacturing processes were applied, this  
6 might be due the different dimensional range between the polymer, acting as a matrix, and the  
7 drug.  
8  
9

10  
11  
12 The representative images of the samples' cross sections are shown in Figure 4. It has been  
13 found that the topology of control specimens (Figure 4A-4B) was comparable to those samples  
14 characterised by a low drug dose (see Figure 4C-4D). The presence of the drug particles was  
15 more evident in the samples loaded with 1% of TC, as can be seen in Figure 4E, and for which  
16 the washing process did not affect the drug retention (Figure 4F).  
17  
18  
19



41  
42 **Figure 4.**  $\mu$ CT cross section images of 0% TC W catheter (A) 0% TC UW catheter (B) 0.25% TC UW  
43 catheter (C) 0.5% TC UW catheter (D) 1% TC UW catheter (E) and 1% TC W catheter (F).  
44

45 Furthermore, it is possible to appreciate the distribution of the drug within the 3D structure  
46 (Figure 5). The presence of the drug in each one of the 3D-printed specimens was assessed by  
47 further analysis and 3D reconstructions. As reported in Figure 5, the distribution of the drug  
48 within the 3D volumes was uniform and proportional to the concentration loaded. Moreover,  
49 even in this case it was demonstrated that the release step (Figure 5F) did not affect the drug  
50 retention, if compared to the UW catheter (Figure 5E).  
51  
52  
53  
54  
55  
56  
57  
58  
59  
60

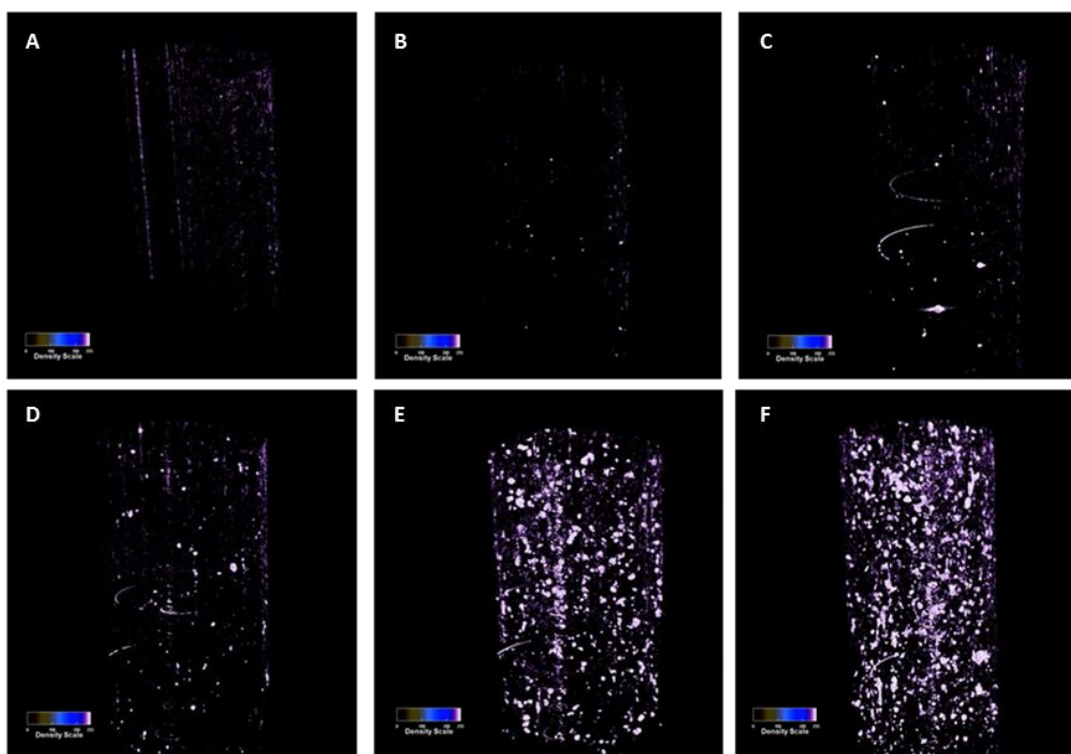


**Figure 5.** 3D reconstruction of the drug distribution in the 3D-printed volume of the 0% TC W catheter (A) 0% TC UW catheter (B) 0.25% TC UW catheter (C) 0.5% TC UW catheter (D) 1% TC UW catheter (E) and 1% TC W catheter (F).

### 3.3. Release Studies

Drug release from catheter structures was analysed using UV analysis. A similar pattern of release was followed by the concentration of drug at 0.25% TC and 0.5% TC (Figure 6). There is an initial burst release of TC released in the first day and then the amount released begins to plateau after the third day. However, catheters containing 1% of TC had a much higher amount of TC released initially compared to the previous ones ( $p < 0.05$ ). At the end of the ten days, there is still an increasing level of TC release for the catheters containing 1% of TC. Although these catheters had a much larger release of TC, this was around 4% release of the total loaded drug after ten days.



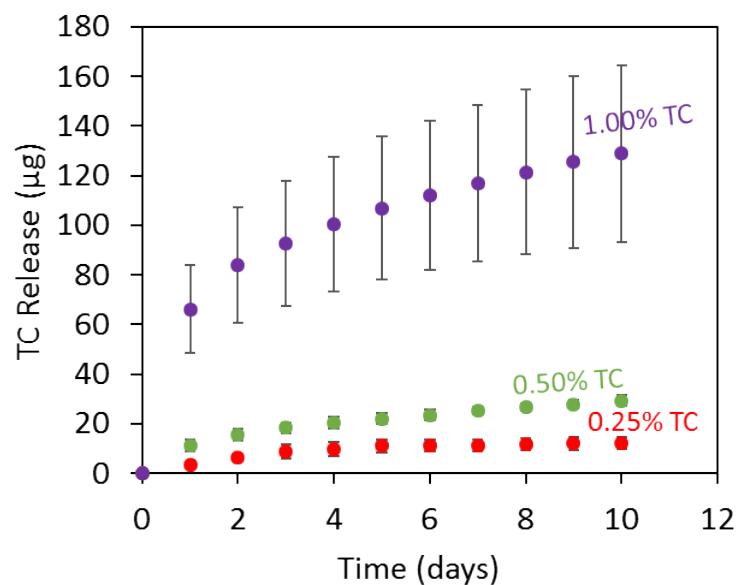


**Figure 6.** Cumulative TC release from 3D-printed catheters containing 0.25%, 0.5% and 1% of TC (Means  $\pm$  S.D; n = 3).

The initial burst release of drug from all of the catheters may be due to the presence of TC on the surface of the catheters. The TC present in the outermost layers of the catheter constructs would have a smaller diffusion distance into the surrounding medium and so may have caused the initial burst release of drug. The abovementioned PLA catheters containing gentamicin sulphate (GS) or methotrexate (MTX) showed a similar pattern to the present study, an initial burst release during the first few hours followed by a steady release.<sup>24</sup>

After ten days, the catheter containing 1% of TC was still releasing and only 4% of the drug was released. This sustained drug release profile may be due to the hydrophobic nature (Figure 1G) of the TPU polymer, which would therefore slow water penetration into polymer matrix. Therefore, this catheter has potential to have prolonged antibacterial effects, as it will be discussed in the following section.

### 3.4. *In Vitro* Microbiological Analysis

Printed catheters were tested for antimicrobial effect on a bacterial culture of *S. aureus*. UW catheters and W catheters were used for this assay. The results of the zone of inhibition are presented in the Figure 7A-7B. A zone of inhibition indicates that *S. aureus* either at the surface of the catheters or even for an area extending outwards from the catheters surface are inhibited. Both, UW and W catheters containing TC exhibited zones of inhibition. As expected, the control catheters containing no TC had no zones of inhibition. The zones of inhibition were increased by increasing the amount of TC. However, statistical analysis showed that there were no significant

differences between the zones of inhibition caused by UW catheters containing 0.25% and 0.5% TC, and the same was observed for W catheters at the same concentrations. ( $p > 0.05$ ). Therefore, it can be inferred that increase in TC concentration from 0.25% to 0.5% did not have a significant impact on the zones of inhibition produced. However, there was a clear increase in the zone of inhibition from 0.25% to 1% ( $p < 0.05$ ) for both UW and W catheters.

On the other hand, comparing UW with W catheters, at 0.25% and 0.5% TC concentrations, there was a decrease in the zones of inhibition after ten days releasing TC in PBS ( $p < 0.05$ ). The average zone of inhibition for W catheters at 0.25% and 0.5% TC concentrations were 6.0 and 7.6 mm, respectively, compared to 9.3 mm and 11.5 mm before the releasing step (UW catheters). Therefore, less TC is diffusing out of the W catheters compared to the UW ones. Nevertheless, there was no significant differences between the halos found for both UW and W catheters at 1% TC ( $p > 0.05$ ), which is in line with the obtained drug release profile for the catheters containing 1% of TC.

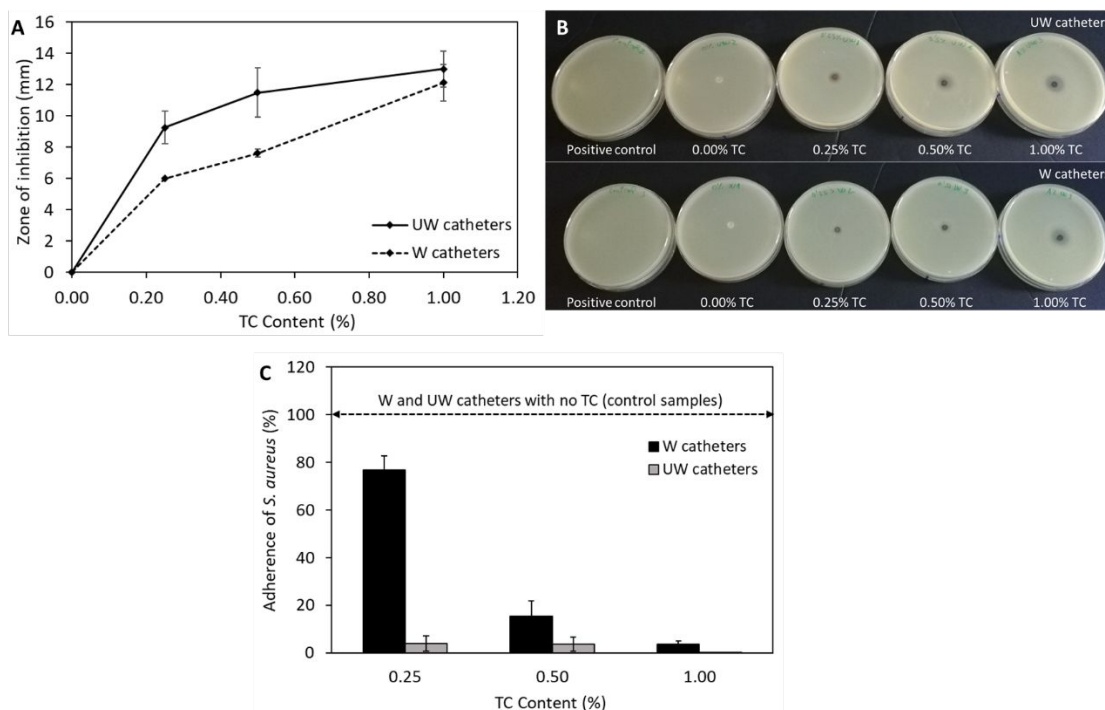


**Figure 7.** Correlation between the diameter of the inhibition zone of *S. aureus* and the concentration of TC (A). Positive *S. aureus* control and agar plates showing zones of inhibition of UW and W catheters (B). Microbial adherence (%) of *S. aureus* to UW and W catheters after 24 h at 37°C p(HEMA) and copolymers of 2-HEMA and conjugates1–3 relative to the p(HEMA) homopolymer, denoted control, after 4 and 24 h incubation at 37°C. Columns and error bars represent means  $\pm$  SD ( $n=3$ ).

1  
2  
3 It is clear that the catheters had bacteriostatic activity on the *S. aureus* culture (Figure 7A-7B).  
4 This further supports the hypothesis that extrusion and 3D-printing did not affect the  
5 bacteriostatic activity of this drug. Catheters containing 0.25% and 0.5% TC had lower  
6 bacteriostatic activity after the ten-day releasing step. This is due to the release of TC during this  
7 step, which would have resulted in the majority of drug on the outer layers of the catheters to  
8 have diffused out. Furthermore, catheters containing 1% TC still had significant bacteriostatic  
9 activity after the release study. It matched the conclusions of this release study as drug was still  
10 being eluted from the catheter after ten days. This drug concentration (1%) is relatively low,  
11 however, it was still able to produce significant zones of inhibition. An issue that exists with  
12 current coated catheters is the risk of toxicity. The ability to use such small quantities of drug  
13 and still have bacteriostatic activity minimises the risk of these drug impregnated catheters  
14 causing toxicity in the patient. Genina *et al.*<sup>59</sup> reported the possibility to print drug-loaded  
15 intrauterine devices using different grades of ethylene vinyl acetate (EVA) and higher percentage  
16 of drugs (5 and 15% of indomethacin). Weisman *et al.*<sup>23</sup> conducted a study on 3D-printed  
17 antibiotic and chemotherapeutic constructs in which 1% and 2.5% gentamicin was used. The 1%  
18 disc tested in bacterial culture of *E. coli* had a similar zone of inhibition (12.9 mm) to 1% TC  
19 catheter in this study (13.0 mm). It is well known that these results depend on the bacteria strain  
20 used, the amount of it, as well as the type of drug. For instance, in this study 80  $\mu$ l of a *S. aureus*  
21 culture were used compared with the 50  $\mu$ l used in the previous work.<sup>23</sup>

22  
23  
24  
25  
26  
27  
28  
29  
30  
31  
32  
33  
34  
35  
36 In addition to the zone of inhibition assay, another *in vitro* assay to study the capacity to avoid  
37 a biofilm formation on the part of the coated catheters was performed. Bacterial adherence to  
38 the surface of the catheters was studied with a model of opportunistic pathogen as *S. aureus*.<sup>60</sup>  
39 Moreover, *S. aureus* is a common causative agent of medical device and bloodstream  
40 infections.<sup>61</sup>

41  
42  
43  
44  
45  
46  
47  
48  
49  
50  
51  
52  
53  
54  
55  
56  
57  
58  
59  
60  
The results of the efficacy of these catheters in resisting adherence of *S. aureus* relative to the  
control catheters containing no TC are presented in the Figure 7C. The greatest reduction in  
adherence of *S. aureus* was achieved by UW catheters containing 1% TC with adherence reduced  
by a mean value of 99.97% after 24 hours (Figure 7C). Nevertheless, this excellent reduction  
value is followed closely by the UW catheters containing 0.25% and 0.5% TC as well as the W  
catheters containing 1% TC, which showed reduction in bacterial adherence values of 96.01,  
96.37 and 96.33% after 24 h, respectively. These results agreed with those of studies on zone of  
inhibition. W catheters containing 1% TC were able to avoid a biofilm formation even after ten  
days releasing TC. Indeed, there were not significant differences between all the UW catheters

1  
2  
3 and the W catheter containing 1% TC ( $p > 0.05$ ). Moreover, even W catheters containing 0.5%  
4 TC (after ten days releasing TC) showed also good results, in terms of reduction values (84.62%),  
5 similar to those obtained using nalidixic acid.<sup>35</sup> Only W catheters containing small amounts of TC  
6 (0.25%) showed poor reduction values (23.26%). These results are therefore extremely  
7 promising considering that antibacterial materials have potential to be used for biomedical  
8 applications.  
9

10  
11  
12  
13  
14 'Nosocomial' or 'healthcare associated infections' (HCAI) affect patients under medical care in  
15 the different health care facilities, such as hospitals.<sup>62</sup> These infections can occur through the  
16 use of medical devices such as catheters and ventilators employed in modern health care.<sup>63</sup>  
17 According to The *World Health Organization (WHO)*, these infections could affect approximately  
18 15% of all hospitalized patients.<sup>64</sup> Moreover, these infections can be caused by bacteria, viruses  
19 and fungal parasites, however, bacteria are the most common pathogens responsible for HCAI.  
20 Highly resistant bacteria such as Methicillin-resistant *S. aureus* are the cause of large part of  
21 these infections worldwide. This means long stays in the health care facilities while increasing  
22 health care costs.<sup>65</sup> Therefore, these novel 3D-printed antibacterial devices, such as catheters,  
23 have a great potential to minimise the appearance of these HCAI.  
24  
25  
26  
27  
28  
29

#### 30 31 **4. Conclusions**

32  
33 This study demonstrates the potential to incorporate drugs into the 3D-printed manufacture of  
34 medical devices. TC was combined with TPU using single screw HME to yield filaments with the  
35 drug dissolved in the matrix. This was confirmed by SEM and TGA measurements. Moreover, the  
36 addition of up to 1% (w/w) of TC did not influence the mechanical or surface properties of the  
37 resulting material. These filaments were used to successfully prepare catheters via-FDM.  
38  
39

40  
41  
42  
43  
44  
45  
46  
47  
48  
49  
50  
51  
52  
53  
54  
55  
56  
57  
58  
59  
60  
61  
62  
63  
64  
65  
66  
67  
68  
69  
70  
71  
72  
73  
74  
75  
76  
77  
78  
79  
80  
81  
82  
83  
84  
85  
86  
87  
88  
89  
90  
91  
92  
93  
94  
95  
96  
97  
98  
99  
100  
101  
102  
103  
104  
105  
106  
107  
108  
109  
110  
111  
112  
113  
114  
115  
116  
117  
118  
119  
120  
121  
122  
123  
124  
125  
126  
127  
128  
129  
130  
131  
132  
133  
134  
135  
136  
137  
138  
139  
140  
141  
142  
143  
144  
145  
146  
147  
148  
149  
150  
151  
152  
153  
154  
155  
156  
157  
158  
159  
160  
161  
162  
163  
164  
165  
166  
167  
168  
169  
170  
171  
172  
173  
174  
175  
176  
177  
178  
179  
180  
181  
182  
183  
184  
185  
186  
187  
188  
189  
190  
191  
192  
193  
194  
195  
196  
197  
198  
199  
200  
201  
202  
203  
204  
205  
206  
207  
208  
209  
210  
211  
212  
213  
214  
215  
216  
217  
218  
219  
220  
221  
222  
223  
224  
225  
226  
227  
228  
229  
230  
231  
232  
233  
234  
235  
236  
237  
238  
239  
240  
241  
242  
243  
244  
245  
246  
247  
248  
249  
250  
251  
252  
253  
254  
255  
256  
257  
258  
259  
260  
261  
262  
263  
264  
265  
266  
267  
268  
269  
270  
271  
272  
273  
274  
275  
276  
277  
278  
279  
280  
281  
282  
283  
284  
285  
286  
287  
288  
289  
290  
291  
292  
293  
294  
295  
296  
297  
298  
299  
300  
301  
302  
303  
304  
305  
306  
307  
308  
309  
310  
311  
312  
313  
314  
315  
316  
317  
318  
319  
320  
321  
322  
323  
324  
325  
326  
327  
328  
329  
330  
331  
332  
333  
334  
335  
336  
337  
338  
339  
340  
341  
342  
343  
344  
345  
346  
347  
348  
349  
350  
351  
352  
353  
354  
355  
356  
357  
358  
359  
360  
361  
362  
363  
364  
365  
366  
367  
368  
369  
370  
371  
372  
373  
374  
375  
376  
377  
378  
379  
380  
381  
382  
383  
384  
385  
386  
387  
388  
389  
390  
391  
392  
393  
394  
395  
396  
397  
398  
399  
400  
401  
402  
403  
404  
405  
406  
407  
408  
409  
410  
411  
412  
413  
414  
415  
416  
417  
418  
419  
420  
421  
422  
423  
424  
425  
426  
427  
428  
429  
430  
431  
432  
433  
434  
435  
436  
437  
438  
439  
440  
441  
442  
443  
444  
445  
446  
447  
448  
449  
450  
451  
452  
453  
454  
455  
456  
457  
458  
459  
460  
461  
462  
463  
464  
465  
466  
467  
468  
469  
470  
471  
472  
473  
474  
475  
476  
477  
478  
479  
480  
481  
482  
483  
484  
485  
486  
487  
488  
489  
490  
491  
492  
493  
494  
495  
496  
497  
498  
499  
500  
501  
502  
503  
504  
505  
506  
507  
508  
509  
510  
511  
512  
513  
514  
515  
516  
517  
518  
519  
520  
521  
522  
523  
524  
525  
526  
527  
528  
529  
530  
531  
532  
533  
534  
535  
536  
537  
538  
539  
540  
541  
542  
543  
544  
545  
546  
547  
548  
549  
550  
551  
552  
553  
554  
555  
556  
557  
558  
559  
560  
561  
562  
563  
564  
565  
566  
567  
568  
569  
570  
571  
572  
573  
574  
575  
576  
577  
578  
579  
580  
581  
582  
583  
584  
585  
586  
587  
588  
589  
590  
591  
592  
593  
594  
595  
596  
597  
598  
599  
600  
601  
602  
603  
604  
605  
606  
607  
608  
609  
610  
611  
612  
613  
614  
615  
616  
617  
618  
619  
620  
621  
622  
623  
624  
625  
626  
627  
628  
629  
630  
631  
632  
633  
634  
635  
636  
637  
638  
639  
640  
641  
642  
643  
644  
645  
646  
647  
648  
649  
650  
651  
652  
653  
654  
655  
656  
657  
658  
659  
660  
661  
662  
663  
664  
665  
666  
667  
668  
669  
670  
671  
672  
673  
674  
675  
676  
677  
678  
679  
680  
681  
682  
683  
684  
685  
686  
687  
688  
689  
690  
691  
692  
693  
694  
695  
696  
697  
698  
699  
700  
701  
702  
703  
704  
705  
706  
707  
708  
709  
710  
711  
712  
713  
714  
715  
716  
717  
718  
719  
720  
721  
722  
723  
724  
725  
726  
727  
728  
729  
730  
731  
732  
733  
734  
735  
736  
737  
738  
739  
740  
741  
742  
743  
744  
745  
746  
747  
748  
749  
750  
751  
752  
753  
754  
755  
756  
757  
758  
759  
760  
761  
762  
763  
764  
765  
766  
767  
768  
769  
770  
771  
772  
773  
774  
775  
776  
777  
778  
779  
780  
781  
782  
783  
784  
785  
786  
787  
788  
789  
790  
791  
792  
793  
794  
795  
796  
797  
798  
799  
800  
801  
802  
803  
804  
805  
806  
807  
808  
809  
810  
811  
812  
813  
814  
815  
816  
817  
818  
819  
820  
821  
822  
823  
824  
825  
826  
827  
828  
829  
830  
831  
832  
833  
834  
835  
836  
837  
838  
839  
840  
841  
842  
843  
844  
845  
846  
847  
848  
849  
850  
851  
852  
853  
854  
855  
856  
857  
858  
859  
860  
861  
862  
863  
864  
865  
866  
867  
868  
869  
870  
871  
872  
873  
874  
875  
876  
877  
878  
879  
880  
881  
882  
883  
884  
885  
886  
887  
888  
889  
890  
891  
892  
893  
894  
895  
896  
897  
898  
899  
900  
901  
902  
903  
904  
905  
906  
907  
908  
909  
910  
911  
912  
913  
914  
915  
916  
917  
918  
919  
920  
921  
922  
923  
924  
925  
926  
927  
928  
929  
930  
931  
932  
933  
934  
935  
936  
937  
938  
939  
940  
941  
942  
943  
944  
945  
946  
947  
948  
949  
950  
951  
952  
953  
954  
955  
956  
957  
958  
959  
960  
961  
962  
963  
964  
965  
966  
967  
968  
969  
970  
971  
972  
973  
974  
975  
976  
977  
978  
979  
980  
981  
982  
983  
984  
985  
986  
987  
988  
989  
990  
991  
992  
993  
994  
995  
996  
997  
998  
999  
1000

These results showed the potential of FDM for anti-infective catheter manufacturing. This is only one potential application of this technology. This proof of concept study displays how antibacterial catheters can be created to combat catheter related infections associated with

1  
2  
3 dialysis catheters. This is the first study that describes the production of usable anti-infective  
4 catheters using 3D-printing.  
5

6  
7 The methods described in the present paper can be applied to various medical devices and a  
8 range of different drug eluting materials. Further research should be done such as the *in vivo*  
9 evaluation of the catheters to fully test their bioactivity and adverse effects. Moreover,  
10 important aspects such as the sterilisation of such devices should be evaluated. Finally, there  
11 are regulatory questions still open about the use of 3D-printing for medical device production.  
12 However, the US Food and Drug Administration (FDA) has started investigate this potential  
13 technology and has published guidelines for manufacturers on how to use this technology  
14 appropriately.<sup>66</sup>  
15  
16  
17  
18  
19

### 20 21 **Supporting Information:**

22  
23 SEM images of the cross section of blank and TPU containing 1% of TC filaments.  $\mu$ CT  
24 reconstructions of all the types of catheters used in this study.  
25  
26

### 27 **References:**

- 28  
29  
30 (1) Hart, L. R.; Li, S.; Sturgess, C.; Wildman, R.; Jones, J. R.; Hayes, W. 3D Printing of  
31 Biocompatible Supramolecular Polymers and Their Composites. *ACS Appl. Mater.*  
32 *Interfaces* **2016**, *8* (5), 3115–3122. <https://doi.org/10.1021/acsami.5b10471>.  
33  
34 (2) Palaganas, N. B.; Mangadlao, J. D.; de Leon, A. C. C.; Palaganas, J. O.; Pangilinan, K. D.;  
35 Lee, Y. J.; Advincula, R. C. 3D Printing of Photocurable Cellulose Nanocrystal Composite  
36 for Fabrication of Complex Architectures via Stereolithography. *ACS Appl. Mater.*  
37 *Interfaces* **2017**, *9* (39), 34314–34324. <https://doi.org/10.1021/acsami.7b09223>.  
38  
39 (3) Guvendiren, M.; Molde, J.; Soares, R. M. D.; Kohn, J. Designing Biomaterials for 3D  
40 Printing. *ACS Biomater. Sci. Eng.* **2016**, *2* (10), 1679–1693.  
41 <https://doi.org/10.1021/acsbiomaterials.6b00121>.  
42  
43 (4) Ligon, S. C.; Liska, R.; Stampfl, J.; Gurr, M.; Mülhaupt, R. Polymers for 3D Printing and  
44 Customized Additive Manufacturing. *Chem. Rev.* **2017**, *117* (15), 10212–10290.  
45 <https://doi.org/10.1021/acs.chemrev.7b00074>.  
46  
47 (5) Sommer, M. R.; Schaffner, M.; Carnelli, D.; Studart, A. R. 3D Printing of Hierarchical Silk  
48 Fibroin Structures. *ACS Appl. Mater. Interfaces* **2016**, *8* (50), 34677–34685.  
49 <https://doi.org/10.1021/acsami.6b11440>.  
50  
51 (6) Domínguez-Robles, J.; Martin, N.; Fong, M.; Stewart, S.; Irwin, N.; Rial-Hermida, M.;  
52  
53  
54  
55  
56  
57  
58  
59  
60

- 1  
2  
3 Donnelly, R.; Larrañeta, E. Antioxidant PLA Composites Containing Lignin for 3D Printing  
4 Applications: A Potential Material for Healthcare Applications. *Pharmaceutics* **2019**, *11*  
5 (4), 165. <https://doi.org/10.3390/pharmaceutics11040165>.  
6  
7  
8  
9 (7) Jose, R. R.; Rodriguez, M. J.; Dixon, T. A.; Omenetto, F.; Kaplan, D. L. Evolution of Bioinks  
10 and Additive Manufacturing Technologies for 3D Bioprinting. *ACS Biomater. Sci. Eng.*  
11 **2016**, *2* (10), 1662–1678. <https://doi.org/10.1021/acsbiomaterials.6b00088>.  
12  
13  
14 (8) Tofail, S. A. M.; Koumoulos, E. P.; Bandyopadhyay, A.; Bose, S.; O'Donoghue, L.; Charitidis,  
15 C. Additive Manufacturing: Scientific and Technological Challenges, Market Uptake and  
16 Opportunities. *Mater. Today* **2018**, *21* (1), 22–37.  
17 <https://doi.org/10.1016/j.mattod.2017.07.001>.  
18  
19  
20 (9) Murphy, S. V; Atala, A. 3D Bioprinting of Tissues and Organs. *Nat. Biotechnol.* **2014**, *32*  
21 (8), 773–785. <https://doi.org/10.1038/nbt.2958>.  
22  
23  
24 (10) Zhao, H.; Yang, F.; Fu, J.; Gao, Q.; Liu, A.; Sun, M.; He, Y. Printing@Clinic: From Medical  
25 Models to Organ Implants. *ACS Biomater. Sci. Eng.* **2017**, *3* (12), 3083–3097.  
26 <https://doi.org/10.1021/acsbiomaterials.7b00542>.  
27  
28  
29 (11) Jang, J.; Yi, H.-G.; Cho, D.-W. 3D Printed Tissue Models: Present and Future. *ACS*  
30 *Biomater. Sci. Eng.* **2016**, *2* (10), 1722–1731.  
31 <https://doi.org/10.1021/acsbiomaterials.6b00129>.  
32  
33  
34 (12) Sandler, N.; Salmela, I.; Fallarero, A.; Rosling, A.; Khajeheian, M.; Kolakovic, R.; Genina,  
35 N.; Nyman, J.; Vuorela, P. Towards Fabrication of 3D Printed Medical Devices to Prevent  
36 Biofilm Formation. *Int. J. Pharm.* **2014**, *459* (1–2), 62–64.  
37 <https://doi.org/10.1016/j.ijpharm.2013.11.001>.  
38  
39  
40 (13) Gibbs, D. M.; Vaezi, M.; Yang, S.; Oreffo, R. O. Hope versus Hype: What Can Additive  
41 Manufacturing Realistically Offer Trauma and Orthopedic Surgery? *Regen. Med.* **2014**, *9*  
42 (4), 535–549. <https://doi.org/10.2217/rme.14.20>.  
43  
44  
45 (14) Haryńska, A.; Gubanska, I.; Kucinska-Lipka, J.; Janik, H. Fabrication and Characterization  
46 of Flexible Medical-Grade TPU Filament for Fused Deposition Modeling 3DP Technology.  
47 *Polymers (Basel)*. **2018**, *10* (12), 1304. <https://doi.org/10.3390/polym10121304>.  
48  
49  
50 (15) Harris, C. G.; Jursik, N. J. S.; Rochefort, W. E.; Walker, T. W. Additive Manufacturing With  
51 Soft TPU – Adhesion Strength in Multimaterial Flexible Joints. *Front. Mech. Eng.* **2019**, *5*.  
52 <https://doi.org/10.3389/fmech.2019.00037>.  
53  
54  
55  
56  
57  
58  
59  
60

- 1  
2  
3 (16) Tappa, K.; Jammalamadaka, U. Novel Biomaterials Used in Medical 3D Printing  
4 Techniques. *J. Funct. Biomater.* **2018**, *9* (1), 17. <https://doi.org/10.3390/jfb9010017>.  
5  
6  
7 (17) Lin, W.-C.; Yu, D.-G.; Yang, M.-C. Blood Compatibility of Thermoplastic Polyurethane  
8 Membrane Immobilized with Water-Soluble Chitosan/Dextran Sulfate. *Colloids Surfaces*  
9 *B Biointerfaces* **2005**, *44* (2–3), 82–92. <https://doi.org/10.1016/j.colsurfb.2005.05.015>.  
10  
11  
12 (18) Ehler, E.; Sterling, D.; Dusenbery, K.; Lawrence, J. Workload Implications for Clinic  
13 Workflow with Implementation of Three-Dimensional Printed Customized Bolus for  
14 Radiation Therapy: A Pilot Study. *PLoS One* **2018**, *13* (10), e0204944.  
15  
16  
17 <https://doi.org/10.1371/journal.pone.0204944>.  
18  
19  
20 (19) Dancewicz, O. L.; Sylvander, S. R.; Markwell, T. S.; Crowe, S. B.; Trapp, J. V. Radiological  
21 Properties of 3D Printed Materials in Kilovoltage and Megavoltage Photon Beams. *Phys.*  
22 *Medica* **2017**, *38*, 111–118. <https://doi.org/10.1016/j.ejmp.2017.05.051>.  
23  
24  
25 (20) Madamesila, J.; McGeachy, P.; Villarreal Barajas, J. E.; Khan, R. Characterizing 3D Printing  
26 in the Fabrication of Variable Density Phantoms for Quality Assurance of Radiotherapy.  
27 *Phys. Medica* **2016**, *32* (1), 242–247. <https://doi.org/10.1016/j.ejmp.2015.09.013>.  
28  
29  
30 (21) Huang, J.-J.; Ren, J.-A.; Wang, G.-F.; Li, Z.-A.; Wu, X.-W.; Ren, H.-J.; Liu, S. 3D-Printed  
31 “Fistula Stent” Designed for Management of Enterocutaneous Fistula: An Advanced  
32 Strategy. *World J. Gastroenterol.* **2017**, *23* (41), 7489–7494.  
33  
34  
35 <https://doi.org/10.3748/wjg.v23.i41.7489>.  
36  
37  
38 (22) Mathew, E.; Domínguez-Robles, J.; Larrañeta, E.; Lamprou, D. A. Fused Deposition  
39 Modelling as a Potential Tool for Antimicrobial Dialysis Catheters Manufacturing: New  
40 Trends vs. Conventional Approaches. *Coatings* **2019**, *9* (8), 515.  
41  
42  
43 <https://doi.org/10.3390/coatings9080515>.  
44  
45  
46 (23) Weisman, J. A.; Nicholson, J. C.; Tappa, K.; Jammalamadaka, U.; Wilson, C. G.; Mills, D. K.  
47 Antibiotic and Chemotherapeutic Enhanced Three-Dimensional Printer Filaments and  
48 Constructs for Biomedical Applications. *Int. J. Nanomedicine* **2015**, *10*, 357–370.  
49  
50  
51 <https://doi.org/10.2147/IJN.S74811>.  
52  
53  
54 (24) Weisman, J. A.; Ballard, D. H.; Jammalamadaka, U.; Tappa, K.; Sumerel, J.; D’Agostino, H.  
55 B.; Mills, D. K.; Woodard, P. K. 3D Printed Antibiotic and Chemotherapeutic Eluting  
56 Catheters for Potential Use in Interventional Radiology. *Acad. Radiol.* **2019**, *26* (2), 270–  
57  
58  
59 274. <https://doi.org/10.1016/j.acra.2018.03.022>.  
60

- 1  
2  
3 (25) Gosbell, I. B. Diagnosis and Management of Catheter-Related Bloodstream Infections  
4 Due to Staphylococcus Aureus. *Intern. Med. J.* **2005**, *35* (s2), S45–S62.  
5 <https://doi.org/10.1111/j.1444-0903.2005.00979.x>.  
6  
7  
8  
9 (26) Thompson, S.; Wiebe, N.; Klarenbach, S.; Pelletier, R.; Hemmelgarn, B. R.; Gill, J. S.;  
10 Manns, B. J.; Tonelli, M. Catheter-Related Blood Stream Infections in Hemodialysis  
11 Patients: A Prospective Cohort Study. *BMC Nephrol.* **2017**, *18* (1), 357.  
12 <https://doi.org/10.1186/s12882-017-0773-5>.  
13  
14  
15  
16 (27) Kerr, M. *Chronic Kidney Disease in England: The Human and Financial Cost*; 2012.  
17  
18 (28) Facts and Stats, Kidney care UK [https://www.kidneycareuk.org/news-and-](https://www.kidneycareuk.org/news-and-campaigns/facts-and-stats/)  
19 [campaigns/facts-and-stats/](https://www.kidneycareuk.org/news-and-campaigns/facts-and-stats/) (accessed Mar 7, 2019).  
20  
21  
22 (29) Sehmi, S. K.; Noimark, S.; Weiner, J.; Allan, E.; MacRobert, A. J.; Parkin, I. P. Potent  
23 Antibacterial Activity of Copper Embedded into Silicone and Polyurethane. *ACS Appl.*  
24 *Mater. Interfaces* **2015**, *7* (41), 22807–22813. <https://doi.org/10.1021/acsami.5b08665>.  
25  
26  
27  
28 (30) Puperi, D. S.; Kishan, A.; Punske, Z. E.; Wu, Y.; Cosgriff-Hernandez, E.; West, J. L.; Grande-  
29 Allen, K. J. Electrospun Polyurethane and Hydrogel Composite Scaffolds as Biomechanical  
30 Mimics for Aortic Valve Tissue Engineering. *ACS Biomater. Sci. Eng.* **2016**, *2* (9), 1546–  
31 1558. <https://doi.org/10.1021/acsbmaterials.6b00309>.  
32  
33  
34  
35 (31) Arefin, A.; Mcculloch, Q.; Martinez, R.; Martin, S. A.; Singh, R.; Ishak, O. M.; Higgins, E.  
36 M.; Haffey, K. E.; Huang, J.-H.; Iyer, S.; et al. Micromachining of Polyurethane Membranes  
37 for Tissue Engineering Applications. *ACS Biomater. Sci. Eng.* **2018**, *4* (10), 3522–3533.  
38 <https://doi.org/10.1021/acsbmaterials.8b00578>.  
39  
40  
41  
42 (32) Stewart, S.; Domínguez-Robles, J.; Donnelly, R.; Larrañeta, E. Implantable Polymeric Drug  
43 Delivery Devices: Classification, Manufacture, Materials, and Clinical Applications.  
44 *Polymers (Basel)*. **2018**, *10* (12), 1379. <https://doi.org/10.3390/polym10121379>.  
45  
46  
47  
48 (33) Baumann, F.; Bugdayci, H.; Grunert, J.; Keller, F.; Roller, D. Influence of Slicing Tools on  
49 Quality of 3D Printed Parts. *Comput. Aided. Des. Appl.* **2016**, *13* (1), 14–31.  
50 <https://doi.org/10.1080/16864360.2015.1059184>.  
51  
52  
53  
54 (34) Larrañeta, E.; Henry, M.; Irwin, N. J.; Trotter, J.; Perminova, A. A.; Donnelly, R. F. Synthesis  
55 and Characterization of Hyaluronic Acid Hydrogels Crosslinked Using a Solvent-Free  
56 Process for Potential Biomedical Applications. *Carbohydr. Polym.* **2018**, *181*, 1194–1205.  
57 <https://doi.org/10.1016/j.carbpol.2017.12.015>.  
58  
59  
60



- 1  
2  
3 (35) McCoy, C. P.; Irwin, N. J.; Brady, C.; Jones, D. S.; Carson, L.; Andrews, G. P.; Gorman, S. P.  
4 An Infection-Responsive Approach To Reduce Bacterial Adhesion in Urinary Biomaterials.  
5 *Mol. Pharm.* **2016**, *13* (8), 2817–2822.  
6 <https://doi.org/10.1021/acs.molpharmaceut.6b00402>.  
7  
8  
9  
10 (36) Wang, R.; Neoh, K. G.; Shi, Z.; Kang, E.-T.; Tambyah, P. A.; Chiong, E. Inhibition of  
11 Escherichia Coli and Proteus Mirabilis Adhesion and Biofilm Formation on Medical Grade  
12 Silicone Surface. *Biotechnol. Bioeng.* **2012**, *109* (2), 336–345.  
13 <https://doi.org/10.1002/bit.23342>.  
14  
15  
16  
17 (37) Jones, D. S.; McGovern, J. G.; Woolfson, A. D.; Gorman, S. P. Role of Physiological  
18 Conditions in the Oropharynx on the Adherence of Respiratory Bacterial Isolates to  
19 Endotracheal Tube Poly(Vinyl Chloride). *Biomaterials* **1997**, *18* (6), 503–510.  
20 [https://doi.org/10.1016/S0142-9612\(96\)00170-6](https://doi.org/10.1016/S0142-9612(96)00170-6).  
21  
22  
23  
24 (38) Miles, A. A.; Misra, S. S.; Irwin, J. O. The Estimation of the Bactericidal Power of the Blood.  
25 *J Hyg* **1938**, *38*, 732–749.  
26  
27  
28  
29 (39) Elastollan Thermoplastic Polyurethane <https://aerospace.basf.com/elastollan.html>  
30 (accessed Mar 8, 2019).  
31  
32  
33 (40) Chopra, I.; Roberts, M. Tetracycline Antibiotics: Mode of Action, Applications, Molecular  
34 Biology, and Epidemiology of Bacterial Resistance. *Microbiol. Mol. Biol. Rev.* **2001**, *65* (2),  
35 232–260. <https://doi.org/10.1128/MMBR.65.2.232-260.2001>.  
36  
37  
38  
39 (41) Okoli, C. P.; Ofomaja, A. E. Development of Sustainable Magnetic Polyurethane Polymer  
40 Nanocomposite for Abatement of Tetracycline Antibiotics Aqueous Pollution: Response  
41 Surface Methodology and Adsorption Dynamics. *J. Clean. Prod.* **2019**, *217*, 42–55.  
42 <https://doi.org/10.1016/j.jclepro.2019.01.157>.  
43  
44  
45  
46 (42) Christ, J. F.; Aliheidari, N.; Ameli, A.; Pötschke, P. 3D Printed Highly Elastic Strain Sensors  
47 of Multiwalled Carbon Nanotube/Thermoplastic Polyurethane Nanocomposites. *Mater.*  
48 *Des.* **2017**, *131*, 394–401. <https://doi.org/10.1016/j.matdes.2017.06.011>.  
49  
50  
51  
52 (43) Jiang, L.; Su, C.; Ye, S.; Wu, J.; Zhu, Z.; Wen, Y.; Zhang, R.; Shao, W. Synergistic  
53 Antibacterial Effect of Tetracycline Hydrochloride Loaded Functionalized Graphene Oxide  
54 Nanostructures. *Nanotechnology* **2018**, *29* (50), 505102. [https://doi.org/10.1088/1361-](https://doi.org/10.1088/1361-6528/aae424)  
55 [6528/aae424](https://doi.org/10.1088/1361-6528/aae424).  
56  
57  
58  
59 (44) Naik, A. D.; Fontaine, G.; Bellayer, S.; Bourbigot, S. Salen Based Schiff Bases to Flame  
60

- 1  
2  
3 Retard Thermoplastic Polyurethane Mimicking Operational Strategies of Thermosetting  
4 Resin. *RSC Adv.* **2015**, *5* (60), 48224–48235. <https://doi.org/10.1039/C5RA06242J>.
- 5  
6  
7 (45) Law, K.-Y. Definitions for Hydrophilicity, Hydrophobicity, and Superhydrophobicity:  
8 Getting the Basics Right. *J. Phys. Chem. Lett.* **2014**, *5* (4), 686–688.  
9 <https://doi.org/10.1021/jz402762h>.
- 10  
11  
12 (46) Maki, D. G.; Cobb, L.; Garman, J. K.; Shapiro, J. M.; Ringer, M.; Helgerson, R. B. An  
13 Attachable Silver-Impregnated Cuff for Prevention of Infection with Central Venous  
14 Catheters: A Prospective Randomized Multicenter Trial. *Am. J. Med.* **1988**, *85* (3), 307–  
15 314. [https://doi.org/10.1016/0002-9343\(88\)90579-7](https://doi.org/10.1016/0002-9343(88)90579-7).
- 16  
17  
18 (47) Hasaniya, N. W. M. A.; Angelis, M.; Brown, M. R.; Yu, M. Efficacy of Subcutaneous Silver-  
19 Impregnated Cuffs in Preventing Central Venous Catheter Infections. *Chest* **1996**, *109* (4),  
20 1030–1032. <https://doi.org/10.1378/chest.109.4.1030>.
- 21  
22  
23 (48) Chen, Y.; Dai, A.; Shi, Y.; Liu, Z.; Gong, M.; Yin, X. Effectiveness of Silver-Impregnated  
24 Central Venous Catheters for Preventing Catheter-Related Blood Stream Infections : A  
25 Meta-Analysis. *Int. J. Infect. Dis.* **2014**, *29*, 279–286.  
26 <https://doi.org/10.1016/j.ijid.2014.09.018>.
- 27  
28  
29 (49) Galloway, S.; Bodenham, A. Long-Term Central Venous Access. *Br. J. Anaesth.* **2004**, *92*  
30 (5), 722–734. <https://doi.org/10.1093/bja/ae109>.
- 31  
32  
33 (50) Moretti, E. W.; Ofstead, C. L.; Kristy, R. M.; Wetzler, H. P. Impact of Central Venous  
34 Catheter Type and Methods on Catheter-Related Colonization and Bacteraemia. *J. Hosp.*  
35 *Infect.* **2005**, *61* (2), 139–145. <https://doi.org/10.1016/j.jhin.2005.02.012>.
- 36  
37  
38 (51) Scott-Warren, V.; Morley, R. Paediatric Vascular Access. *BJA Educ.* **2015**, *15* (4), 199–206.  
39 <https://doi.org/10.1093/bjaceaccp/mku050>.
- 40  
41  
42 (52) Liu, Z.; Wang, Y.; Wu, B.; Cui, C.; Guo, Y.; Yan, C. A Critical Review of Fused Deposition  
43 Modeling 3D Printing Technology in Manufacturing Polylactic Acid Parts. *Int. J. Adv.*  
44 *Manuf. Technol.* **2019**, *102* (9–12), 2877–2889. [https://doi.org/10.1007/s00170-019-](https://doi.org/10.1007/s00170-019-03332-x)  
45 [03332-x](https://doi.org/10.1007/s00170-019-03332-x).
- 46  
47  
48 (53) Lalehpour, A.; Barari, A. Post Processing for Fused Deposition Modeling Parts with  
49 Acetone Vapour Bath. *IFAC-PapersOnLine* **2016**, *49* (31), 42–48.  
50 <https://doi.org/10.1016/j.ifacol.2016.12.159>.
- 51  
52  
53 (54) Zhao, G.; Ma, G.; Feng, J.; Xiao, W. Nonplanar Slicing and Path Generation Methods for  
54  
55  
56  
57  
58  
59  
60

- 1  
2  
3           Robotic Additive Manufacturing. *Int. J. Adv. Manuf. Technol.* **2018**, *96* (9–12), 3149–3159.  
4           <https://doi.org/10.1007/s00170-018-1772-9>.  
5  
6  
7           (55) Alhers, D. 3D Printing of Nonplanar Layers for Smooth Surface Generation, Universität  
8           Hamburg, 2018.  
9  
10  
11           (56) Macha, I. J.; Ben-Nissan, B.; Vilchevskaya, E. N.; Morozova, A. S.; Abali, B. E.; Müller, W.  
12           H.; Rickert, W. Drug Delivery From Polymer-Based Nanopharmaceuticals—An  
13           Experimental Study Complemented by Simulations of Selected Diffusion Processes.  
14           *Front. Bioeng. Biotechnol.* **2019**, *7*. <https://doi.org/10.3389/fbioe.2019.00037>.  
15  
16  
17           (57) Kaur, G.; Grewal, J.; Jyoti, K.; Jain, U. K.; Chandra, R.; Madan, J. Oral Controlled and  
18           Sustained Drug Delivery Systems. In *Drug Targeting and Stimuli Sensitive Drug Delivery*  
19           *Systems*; Elsevier, 2018; pp 567–626. [https://doi.org/10.1016/B978-0-12-813689-](https://doi.org/10.1016/B978-0-12-813689-8.00015-X)  
20           8.00015-X.  
21  
22           (58) Goyanes, A.; Fina, F.; Martorana, A.; Sedough, D.; Gaisford, S.; Basit, A. W. Development  
23           of Modified Release 3D Printed Tablets (Printlets) with Pharmaceutical Excipients Using  
24           Additive Manufacturing. *Int. J. Pharm.* **2017**, *527* (1–2), 21–30.  
25           <https://doi.org/10.1016/j.ijpharm.2017.05.021>.  
26  
27           (59) Genina, N.; Holländer, J.; Jukarainen, H.; Mäkilä, E.; Salonen, J.; Sandler, N. Ethylene Vinyl  
28           Acetate (EVA) as a New Drug Carrier for 3D Printed Medical Drug Delivery Devices. *Eur.*  
29           *J. Pharm. Sci.* **2016**, *90*, 53–63. <https://doi.org/10.1016/j.ejps.2015.11.005>.  
30  
31           (60) Larrañeta, E.; Imízcoz, M.; Toh, J. X.; Irwin, N. J.; Ripolin, A.; Perminova, A.; Domínguez-  
32           Robles, J.; Rodríguez, A.; Donnelly, R. F. Synthesis and Characterization of Lignin  
33           Hydrogels for Potential Applications as Drug Eluting Antimicrobial Coatings for Medical  
34           Materials. *ACS Sustain. Chem. Eng.* **2018**, *6* (7), 9037–9046.  
35           <https://doi.org/10.1021/acssuschemeng.8b01371>.  
36  
37           (61) Tong, S. Y. C.; Davis, J. S.; Eichenberger, E.; Holland, T. L.; Fowler, V. G. Staphylococcus  
38           Aureus Infections: Epidemiology, Pathophysiology, Clinical Manifestations, and  
39           Management. *Clin. Microbiol. Rev.* **2015**, *28* (3), 603–661.  
40           <https://doi.org/10.1128/CMR.00134-14>.  
41  
42           (62) Khan, H. A.; Baig, F. K.; Mehboob, R. Nosocomial Infections: Epidemiology, Prevention,  
43           Control and Surveillance. *Asian Pac. J. Trop. Biomed.* **2017**, *7* (5), 478–482.  
44           <https://doi.org/10.1016/j.apjtb.2017.01.019>.  
45  
46  
47  
48  
49  
50  
51  
52  
53  
54  
55  
56  
57  
58  
59  
60

- 1  
2  
3 (63) CDC. Types of healthcare-associated infections. Healthcare-associated infections (HAIs)  
4 <https://www.cdc.gov/HAI/infectionTypes.html> (accessed Mar 10, 2019).  
5  
6  
7 (64) Sydnor, E. R. M.; Perl, T. M. Hospital Epidemiology and Infection Control in Acute-Care  
8 Settings. *Clin. Microbiol. Rev.* **2011**, *24* (1), 141–173.  
9 <https://doi.org/10.1128/CMR.00027-10>.  
10  
11  
12 (65) Hall, C. W.; Mah, T.-F. Molecular Mechanisms of Biofilm-Based Antibiotic Resistance and  
13 Tolerance in Pathogenic Bacteria. *FEMS Microbiol. Rev.* **2017**, *41* (3), 276–301.  
14 <https://doi.org/10.1093/femsre/fux010>.  
15  
16  
17 (66) Statement by FDA Commissioner Scott Gottlieb, M.D., on FDA ushering in new era of 3D  
18 printing of medical products; provides guidance to manufacturers of medical devices  
19 [https://www.fda.gov/news-events/press-announcements/statement-fda-](https://www.fda.gov/news-events/press-announcements/statement-fda-commissioner-scott-gottlieb-md-fda-ushering-new-era-3d-printing-medical-products)  
20 [commissioner-scott-gottlieb-md-fda-ushering-new-era-3d-printing-medical-products](https://www.fda.gov/news-events/press-announcements/statement-fda-commissioner-scott-gottlieb-md-fda-ushering-new-era-3d-printing-medical-products)  
21 (accessed Mar 15, 2019).  
22  
23  
24  
25  
26  
27  
28  
29  
30  
31  
32  
33  
34  
35  
36  
37  
38  
39  
40  
41  
42  
43  
44  
45  
46  
47  
48  
49  
50  
51  
52  
53  
54  
55  
56  
57  
58  
59  
60

## Fused Deposition Modelling as an Effective Tool for Anti-Infective Dialysis Catheter Fabrication

Essyrose Mathew,<sup>1,1</sup> Juan Domínguez-Robles,<sup>1,1</sup> Sarah A. Stewart,<sup>1</sup> Elena Mancuso,<sup>2</sup> Kieran O'Donnell,<sup>2</sup> Eneko Larrañeta,<sup>1</sup> Dimitrios A. Lamprou<sup>1</sup>

<sup>1</sup> School of Pharmacy, Queen's University Belfast, 97 Lisburn Road, Belfast BT9 7BL, UK

<sup>2</sup> Nanotechnology and Integrated Bio-Engineering Centre (NIBEC), Ulster University, Jordanstown campus, UK

### Table of Content

